

# Physicochemical Studies on the Interaction between *N*-Decanoyl-*N*-methylglucamide and Bovine Serum Albumin

C. Carnero Ruiz,\* J. M. Hierrezuelo, J. Aguiar, and J. M. Peula-García

*Grupo de Fluidos Estructurados y Sistemas Anfífilos, Departamento de Física Aplicada II, Escuela Universitaria Politécnica, Universidad de Málaga, Campus de El Ejido, 29013 Málaga, Spain*

*Received April 16, 2007; Revised Manuscript Received June 4, 2007*

The protein–surfactant system constituted by bovine serum albumin (BSA) and *N*-decanoyl-*N*-methylglucamide (MEGA-10) has been studied by using surface tension, steady-state fluorescence, and dynamic light scattering measurements. It was found that the presence of protein delays the surfactant aggregation, which was interpreted as a sign of binding between surfactant and protein. Binding studies were carried out by two different methods. First, a treatment based on surface tension measurements was used to obtain information on the number of surfactant molecules bound per protein molecule under saturation conditions. Second, the binding curve for the BSA/MEGA-10 system was determined by examining the behavior of the intrinsic BSA fluorescence upon the surfactant addition. Both approaches indicate that the binding process is essentially cooperative in nature. The results of the aggregation numbers of MEGA-10 micelles, as well as those of resonance energy transfer from tryptophan residues to 8-anilino-1-naphthalene-sulfonate, corroborate the formation of micelle-like aggregates of surfactants, smaller than the free micelles, adsorbed on the protein surface. The dynamic light scattering results were not conclusive, in the sense that it was not possible to discriminate between protein–surfactant complexes and free micelles. However, the overall results suggest the formation of “pearl necklace” complexes in equilibrium with the free micelles of the surfactant.

## Introduction

Because of their ability to catalyze biochemical reactions, to be adsorbed on the surface of some substances, and to bind other molecules and form molecular aggregates, globular proteins are frequently used as functional ingredients in health care and pharmaceutical products.<sup>1</sup> Bovine serum albumin (BSA) is an important globular protein that has been widely used as a model for studying the interaction between proteins and different substrates.<sup>2</sup> Many amphiphilic molecules, such as surfactants, are known to interact with peptides and proteins, being that these interactions are of great importance not only in vivo but also in several technical applications.<sup>3</sup> Therefore, studies on the interactions between proteins and surfactants in aqueous medium, as well as on the structures of the complexes formed as a result of those interactions, have been extensively reviewed.<sup>4–6</sup>

With regards to their ability for interacting with proteins, ionic surfactants are more effective than nonionic ones. It is well-known that the charged group of anionic surfactants interacts electrostatically with the oppositely charged group of the amino acids causing denaturation of the protein.<sup>7</sup> Therefore, much experimental work has been made for studying the interaction between proteins and sodium dodecyl sulfate (SDS) and other anionic surfactants, being that the studies involving cationic and nonionic surfactants are rather scarce.<sup>7–14</sup> However, as mentioned previously, the ionic surfactants can produce significant conformational alterations in the protein structure with subsequent changes in its functionality. Because these modifications are undesirable in many applications, the use of nonionic surfactants is preferred. In addition, due to their favorable physicochemical properties, nonionic surfactants are extensively

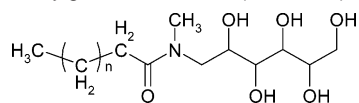
used in many fields of technology and research, including pharmaceutical preparations, where these substances increase the stability and dissolution rate of many active ingredients. The interactions involved in the binding of ethoxylated nonionic surfactants to proteins are being characterized. From these investigations, it can be concluded that the hydrophobic moiety of surfactants can bind to the apolar amino acids, whereas the hydrophilic ethyleneoxide chain can interact with the peptide bond and with one or more polar amino acids residues, probably by electrostatic interactions and hydrogen bonding.<sup>15</sup>

Recently, a relatively new class of nonionic surfactants, so-called sugar-based surfactants, is emerging due to advantages with regard to performance, health of consumers, and environmental compatibility as compared to the more common ethoxylated nonionic surfactants.<sup>16</sup> *N*-Decanoyl-*N*-methylglucamide (MEGA-10) (see Scheme 1) is an important member of this family, belonging to the group of fatty acid glucamides, which has been used as a membrane protein solubilizer since it was synthesized by Hildreth, as this surfactant seems to maintain protein functions.<sup>17</sup> Nevertheless, as far as we know, the nature of the interaction between MEGA-10 and proteins appears not to have been studied. Therefore, we have decided to examine this system. In this paper, the interaction between nonionic MEGA-10 surfactant and BSA has been investigated by using tensiometry, steady-state fluorescence, and dynamic light scattering. We have focused our attention on two aspects: the nature of the binding between protein and surfactant and the characterization of the protein–surfactant complexes.

## Experimental Procedures

**Materials.** The samples of MEGA-10 and BSA used in this work were acquired from Sigma, and due to their high purity grade, these materials were used without further purification. All solutions were

\* Corresponding author. E-mail: ccarnero@uma.es.

**Scheme 1.** Molecular Structure of *N*-Decanoyl-*N*-methylglucamide,  $n = 7$  (MEGA-10)

prepared in a glycine-HCl buffer of ionic strength 0.1 M in NaCl at pH 5.75. The fluorescence probes pyrene and 8-anilinoanthracene-1-sulfonate (ANS) were purchased from Sigma and Fluka, respectively, and were also used as received. The quencher cetylpyridinium chloride (CPyC) was also delivered by Sigma. Stock solutions (1 mM) of the fluorescence probes were prepared in absolute ethanol and stored at 4 °C. From these solutions, work solutions of a lower concentration were prepared by dilution. All measurements were carried out with freshly prepared solutions. All chemicals used were of analytical grade quality. Ultrapure water for the preparation of the solutions (resistivity  $\sim 18$  M $\Omega$  cm) was obtained by passing deionized water through an ultrahigh quality polishing system (UHQ-PS, ELGA). All percentage concentrations of BSA given in this paper are expressed in weight per volume.

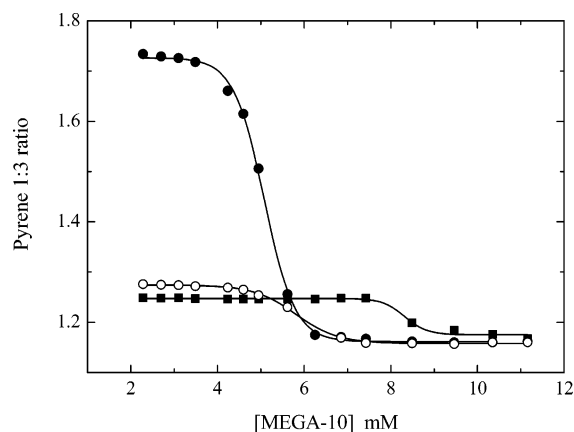
**Tensiometry.** The measurements of surface tension were made using the ring method with a Sigma 701 (KSV) tensiometer. The solutions were thermostated at 30 °C by a circulating water bath. The ring was cleaned with distilled water and acetone and, finally, flamed. Sets of measurements were made by the dilution method, that is, different volumes of buffer or buffered protein solutions were added to a concentrated surfactant solution containing the same protein concentration. After each dilution, the resultant solution was stabilized for at least 15 min before carrying out the measurement. The surface tension values were accurate within  $\pm 0.1$  mN  $m^{-1}$ .

**Spectrofluorometry.** Fluorescence measurements were made on a SPEX FluoroMax-2 spectrofluorometer in the "S" mode. This apparatus was equipped with a thermostated cell housing and fitted with a 150 W xenon lamp and 1 cm  $\times$  1 cm quartz cells. All fluorescence measurements were made at  $30.0 \pm 0.1$  °C.

The aggregation process of the surfactant in either the absence or the presence of protein was followed by the pyrene 1:3 ratio method.<sup>18</sup> Briefly, fluorescence emission spectra of different surfactant solutions containing around 1  $\mu$ M pyrene and a fixed protein concentration were recorded between 360 and 500 nm by using an excitation wavelength of 335 nm and bandwidth of 1.00 nm. From these spectra, intensities  $I_1$  and  $I_3$  were measured at the wavelengths corresponding to the first and third vibronic bands located near 373 and 384 nm. The ratio  $I_1/I_3$  is the so-called pyrene 1:3 ratio index.

The steady-state fluorescence quenching method<sup>19</sup> was used to determine the mean micellar aggregation number ( $N_{agg}$ ). In all the quenching experiments, pyrene was used as a luminescence probe and CPyC as a quencher. Stock solutions containing pyrene (3  $\mu$ M), and surfactant (90 mM), were prepared in either buffer solution or protein solutions of different concentrations. Working solutions of lower concentrations (1  $\mu$ M in pyrene and 30 mM in surfactant) were prepared by adding appropriate volumes of quencher solutions. In these studies, the quencher concentrations employed were maintained low enough ( $< 0.18$  mM) so as not to interfere with the assembly of the surfactant. From these solutions, fluorescence intensities were recorded by using excitation and emission wavelengths of 335 and 383 nm, respectively. Triplicate experiments were carried out for each system with different protein contents. The errors in  $N_{agg}$ , in terms of the standard deviation of three individual determinations, are estimated to be less than 3%.

To analyze how the presence of surfactant affects to the protein structure, resonance energy transfer studies from tryptophan (Trp) residues of BSA to the ANS molecule were performed. In these experiments, we used solutions with a fixed protein concentration (30  $\mu$ M), different surfactant concentrations, and increasing concentration of acceptor (ANS). Fluorescence emission spectra of these solutions were recorded by using an excitation wavelength of 295 nm and bandwidth of 2.00 nm. From these spectra, fluorescence intensities corresponding to the peaks of the donor ( $\sim 340$  nm) and acceptor ( $\sim 460$  nm) were measured.

**Figure 1.** Plot of pyrene 1:3 ratio vs concentration of MEGA-10 at different BSA concentrations: (●) 0, (○) 0.1%, and (■) 1.0%.

**Dynamic Light Scattering.** Dynamic light scattering measurements were carried out with a Zetasizer NanoS instrument (Malvern Instruments). This apparatus, which uses backscattering detection (scattering angle  $\theta = 173^\circ$ ) and an avalanche photodiode detector (APD), is equipped with a helium-neon laser source (wavelength 633 nm and power 4.0 mW) and a thermostated sample chamber controlled by a thermoelectric Peltier. In these studies, we used solutions with a fixed protein concentration and increasing surfactant concentrations, ranging from the pre- to post-micellar region. In addition, we also examined the single system constituted of only either BSA (30  $\mu$ M) or MEGA-10 employing a concentration well above the critical micelle concentration (CMC) (15 mM). All these measurements were made at  $30.0 \pm 0.1$  °C.

## Results and Discussion

### Effect of Addition of BSA on Aggregation of MEGA-10.

As stated previously, we have followed the effect of BSA on the aggregation process of the surfactant by two different methods: the pyrene 1:3 ratio method and that based on surface tension measurements. Figure 1 shows the dependence of the pyrene 1:3 ratio index on the surfactant concentration without BSA and with 0.1 and 1% BSA. In this figure, we can see that in all cases the pyrene 1:3 ratio index shows a typical sigmoidal decrease with the surfactant concentration. However, it is observed that in the presence of the protein, when the surfactant concentration is low and the micelles are not formed, pyrene is bound in a hydrophobic site of the protein, where the pyrene 1:3 ratio index is much lower than in water but not as low as in MEGA-10 micelles. However, as soon as micelles are formed, pyrene prefers the micellar hydrophobic environment. It is to be noted that a similar behavior previously has been observed in the BSA/C<sub>12</sub>E<sub>8</sub> system.<sup>20</sup> By using the data treatment previously described,<sup>21</sup> we have obtained a value of 5.1 mM for the CMC of MEGA-10 in the absence of protein. In this case, the experimental data were fitted to a Boltzmann sigmoidal-type curve, the center of the sigmoid being identified as the CMC. However, due to little variation in the pyrene 1:3 ratio index when the protein is present, we have found that the application of this method is highly speculative. From a qualitative point of view, data in Figure 1 indicate that the surfactant aggregation process is delayed as the protein content increases. This fact could be interpreted as evidence of the interaction between surfactant and protein. Note that if the surfactant is adsorbed on the protein surface before aggregation, it seems reasonable that this process begins later when the protein concentration is higher.

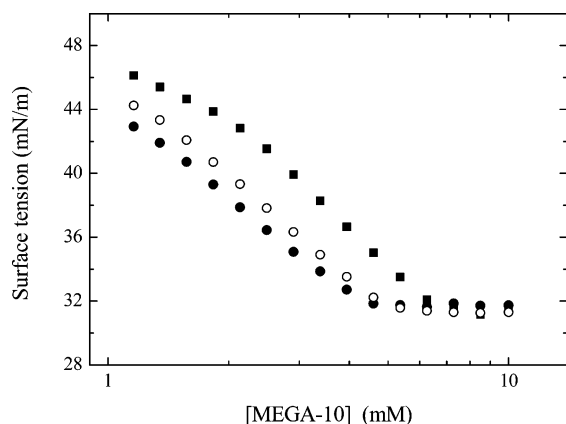


**Figure 2.** Surface tension of MEGA-10 solutions vs total surfactant concentration in the presence of different BSA concentrations: (●) 0, (○) 0.1%, and (■) 1.0%.

**Table 1.** Parameters Obtained from Data Treatment Based on Surface Tension Measurements for BSA/MEGA-10 System at 30.0 °C

BSA (% w/v)	CMC (mM)	$a \times 10^3$ (mmol/m <sup>2</sup> )	$\Gamma_p^0 \times f \times 10^3$ (mmol/m <sup>2</sup> )	$K_s$ (L/mol)	$(C_s)_{\text{sat}}$ (mM)	$(C_s^f)_{\text{sat}}$ (mM)	$\nu_{\text{sat}}$
0	4.4	3.41					
0.1	5.1	3.57	2.29	$1.91 \times 10^4$	5.1	4.4	45.8
1	6.8	4.10	2.44	$1.08 \times 10^4$	6.8	4.4	16.1

Surface tension measurements of MEGA-10 solutions without BSA and with 0.1 and 1% BSA are shown in Figure 2. From this figure, it can be seen that at low surfactant concentrations, the surface tension value is higher in the presence of the protein, indicating that this species is itself surface active. Moreover, it is observed that each plot exhibits a sharp break at each CMC, the surface tension remaining almost constant above this point. Another aspect to be noted is that the surface tension constant value is practically independent of the protein concentration. A similar behavior has been previously observed by several authors in different protein–nonionic surfactant systems.<sup>22–25</sup> Plots in Figure 2 indicate that as the surfactant concentration increases, protein surfactant complexes are formed, and they counteract the surface tension lowering in a dual way (i.e., by consumption of both surfactant and free protein and by the formation of surface inactive complexes).<sup>24</sup> From the break points of the plots in Figure 2, we have obtained the corresponding CMC values (see Table 1). In the absence of protein, we have obtained a value of 4.4 mM, a value slightly lower than that obtained by the pyrene 1:3 ratio method. This is a reasonable result because the probe-based procedure requires the formation of aggregates where the probe can be incorporated.

**Binding of MEGA-10 to BSA.** The binding studies of the surfactant to protein have been performed by two different methods. First, we have employed an approach based on surface tension measurements, and then we obtained the binding curve between surfactant and protein through the change in the intrinsic fluorescence of BSA as the surfactant concentration was increased.

Nishikido et al.<sup>22</sup> have developed a method based on surface tension measurements to obtain the binding isotherm between hydrophilic protein and nonionic surfactants. The method was successfully applied in the systems C<sub>12</sub>E<sub>6</sub>-BSA and C<sub>12</sub>E<sub>6</sub>-lysozyme<sup>22</sup> and Triton X-100-BSA.<sup>23</sup> Later, Nishiyama and Maeda<sup>24</sup> employed a simplified version of that approach to study the binding between several ethoxylated nonionic surfactants and lysozyme. The procedure proposed by Nishikido et al.<sup>22</sup> is based on the assumption that the protein–surfactant complex

is not surface active. These authors proposed an expression for the surface tension of the air–liquid interface containing surfactant and protein,  $\gamma$ , given by

$$\gamma = -aRT \ln[a + K_s(a - \Gamma_p^0)fC_s^f] + \gamma_p + aRT \ln a \quad (1)$$

where  $a$  is the maximum adsorption of surfactant,  $K_s$  is the Langmuir constant for adsorption of the surfactant at the air–liquid interface,  $\Gamma_p^0$  and  $\gamma_p$  refer to the amount of adsorbed protein at the air–liquid interface and the surface tension of solutions containing the same concentration of protein but no surfactant,  $f$  is the ratio between maximum surfactant adsorption and maximum protein adsorption, and  $C_s^f$  is the concentration of surfactant monomer or free surfactant concentration. In the case of a pure surfactant solution, the surface tension is given by

$$\gamma_s = -aRT \ln[1 + K_s C_s^0] + \gamma_{\text{water}} \quad (2)$$

where  $C_s^0$  is the concentration of pure surfactant, and  $\gamma_{\text{water}}$  is the surface tension of pure water.

If we assume that at the surfactant concentration at which  $\gamma$  becomes constant, CMC, the surfactant monomers begin forming micelles, and that the monomer concentration is equal to the CMC of pure surfactant ( $\text{CMC}^0$ ), and taking into account that  $\gamma_{\text{CMC}} = \gamma_{\text{CMC}^0}$ , as observed in the plots of Figure 2, from eqs 1 and 2, one can obtain

$$\gamma_{\text{CMC}} = -aRT \ln[1 + K_s \text{CMC}^0] + \gamma_{\text{water}} \quad (3)$$

$$\Gamma_p^0 f = \frac{a(1 + K_s \text{CMC}^0) \left\{ 1 - \exp\left(-\frac{\gamma_{\text{water}} - \gamma_p}{aRT}\right) \right\}}{K_s \text{CMC}^0} \quad (4)$$

In this manner, by introducing the experimental data of surface tension in eqs 1, 3, and 4, the average number of bound surfactant monomers per protein molecule,  $\nu$ , can be determined by using the relationship

$$\nu = \frac{C_s - C_s^f}{C_p} \quad (5)$$

where  $C_s$  is the total surfactant concentration. The procedure consists of obtaining  $a$  from the slope of the isotherm adsorption in the air–liquid interface, in the pre-micellar region, according to the Gibbs adsorption equation.<sup>26</sup> Then,  $K_s$  may be determined introducing in eq 3 the values of  $a$ ,  $\text{CMC}^0$ , and  $\gamma_{\text{water}}$ . After obtaining  $\Gamma_p^0 f$  from eq 4,  $C_s^f$  can be finally calculated by applying eq 1. Once  $C_s^f$  is determined, one can estimate the average number of bound surfactant monomers per protein molecule,  $\nu$ , from eq 5.

In Figure 3, we show a representative plot of the free surfactant concentration against the total surfactant concentration in the presence of 0.1% BSA, as obtained by applying the previous treatment to the experimental data in Figure 2. Data in Figure 3 indicate that the concentration of free surfactant,  $C_s^f$ , increases linearly with the total surfactant concentration until reaching a saturation value,  $(C_s^f)_{\text{sat}}$ , which can be determined by the intersection of the two straight lines, as indicated in Figure 3. Then, the saturation average number of bound surfactant monomers per protein molecule,  $\nu_{\text{sat}}$ , can be estimated. Table 1 summarizes all the parameters that we have obtained by using the procedure based on the surface tension measurements. Data



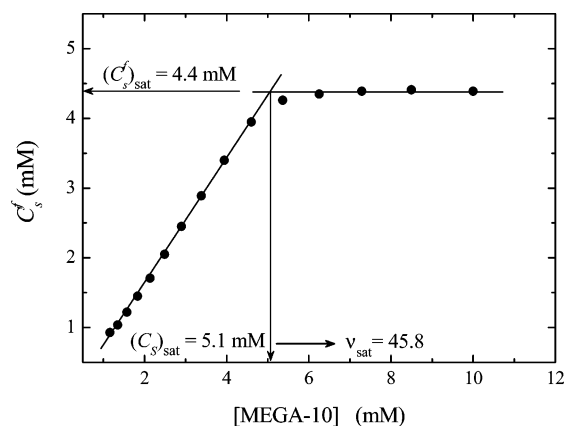


**Figure 3.** Free surfactant concentration,  $C_s^f$ , vs total surfactant concentration in the presence of 0.1% BSA.

in Table 1 indicate that both the constant,  $K_s$ , and the maximum number of bound surfactants per protein molecule are greater the smaller the protein concentration is, in good agreement with observations of Nishikido et al. for the BSA/C<sub>12</sub>E<sub>6</sub> system.<sup>22</sup> The fact that  $\nu_{\text{sat}}$  decreases with protein concentration is probably due to that the number of hydrophobic regions of proteins, which are surfactant binding sites, can be hidden as a result of the protein–protein interactions within the protein aggregates, this process being effectively enhanced by the increase in protein concentration.<sup>22</sup> Therefore, it may be anticipated that the  $\nu_{\text{sat}}$  value obtained at high protein concentrations is probably underestimated. On the other hand, the model of Nishikido et al.<sup>22</sup> assumes that at the surfactant concentration where the surface tension begins to stay constant, surfactant monomers begin to form micelles, and the concentration of monomers remains identical with the CMC of the surfactant alone, as illustrated in Figure 3. At this moment, the saturation occurs, and hence, the added surfactant is employed in forming free micelles but is not adsorbed on the protein. This fact reinforces the idea that the saturation values of  $\nu$  reported by the present procedure are probably underestimated. Nevertheless, the values obtained by  $\nu_{\text{sat}}$  suggest the formation of surfactant clusters adsorbed on the protein surface, according to a mechanism cooperative in nature. However, since the  $\nu_{\text{sat}}$  values are smaller than the micelle aggregation number of MEGA-10, it seems that the mechanism controlling the binding of MEGA-10 to BSA differs from that governing the micelle formation.

On the other hand, to obtain additional information on the binding of surfactant to protein, we have used an alternative method based on the effect of the surfactant addition on the intrinsic fluorescence of BSA. With this purpose, the fluorescence of tryptophan (Trp) residues, with excitation at 295 nm, was monitored at different surfactant concentrations at a fixed protein concentration (30  $\mu\text{M}$ ). The fractional change of protein fluorescence due to surfactant binding,  $\theta$ , was calculated as<sup>9,27</sup>

$$\theta = \frac{I_{\text{obs}} - I_f}{I_{\text{min}} - I_f} \quad (6)$$

where  $I_{\text{obs}}$  is the fluorescence intensity at any surfactant concentration,  $I_f$  is the fluorescence intensity in the absence of surfactant, and  $I_{\text{min}}$  is the fluorescence intensity under saturation binding conditions. It is to be remarked that this procedure does not measure the number of surfactant molecules bound to protein,  $\nu$ , but provides the fraction of a BSA molecule bound by surfactant.<sup>27</sup> That is, if a BSA molecule has  $n_0$  binding sites and at a certain stage surfactant molecules bind to  $n$  sites, then

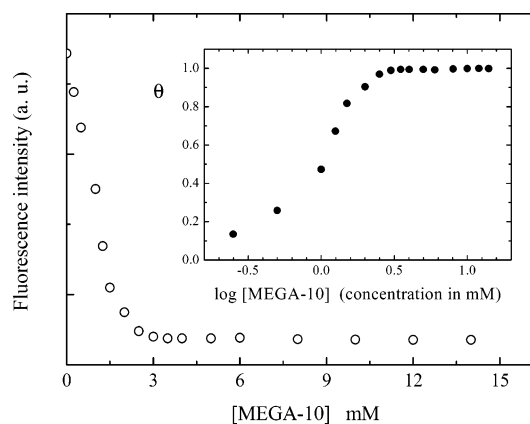


**Figure 4.** Intrinsic fluorescence of BSA (30  $\mu\text{M}$ ) as a function of the total surfactant concentration. Inset: binding curve, showing the fraction of a protein molecule bound by surfactant ( $\theta$ ) as a function of the log of total surfactant concentration for the interaction between BSA and MEGA-10.

the fraction of BSA bound to surfactant is  $\theta = n/n_0$ . Therefore, in the absence of surfactant  $\theta = 0$ , and when the saturation is reached and all the possible sites of BSA are occupied by surfactants,  $\theta = 1$ , and after that, no further interaction between protein and surfactant takes place.<sup>9</sup> This remark is very important; note that recently the present procedure has been erroneously applied to the estimation of the number of surfactant molecules bound per protein molecule.<sup>28–30</sup>

Figure 4 shows the intrinsic fluorescence intensity of BSA as a function of MEGA-10 concentration. It is observed that binding of surfactant is accompanied by quenching of the intrinsic protein fluorescence; however, no spectral shape changes indicating denaturation were observed. It is well-known that Trp fluorescence decreases upon exposure to a polar environment;<sup>31</sup> therefore, it can be postulated that the binding of surfactant on protein causes some conformational change in the protein structure, resulting in a greater exposure of Trp residues to the aqueous environment. In Figure 4, we also show the binding curve for the BSA/MEGA-10 system as obtained by the parameter  $\theta$  as a function of the total surfactant concentration. In general, the binding isotherm of a surfactant, for example, SDS, onto a protein is characterized by the existence of four regions. In the initial region, at the lowest surfactant concentration, there is some binding to specific high-energy sites on the protein. This region is followed by either a plateau or a slow rising part, where the binding of non-cooperative characters occurs. Beyond that, a third region where a massive increase in binding due to cooperative interactions takes place is observed. Finally, the binding curve shows a plateau, indicating that further binding of the surfactant does not occur on the protein and that the free micelles are formed as excess surfactant is added; this is the so-called saturation region.<sup>7,32</sup> According to this scheme, the binding curve between MEGA-10 and BSA (inset in Figure 4) can be interpreted as follows. The specific binding region appears to be absent; this is evidently due to the nonionic character of MEGA-10. The second and third regions are not clearly demarcated; at low surfactant concentrations, a slight increase of  $\theta$  that immediately undergoes a considerable increase with the surfactant concentration is observed. We think that our data indicate a non-cooperative binding process at low surfactant concentrations, controlled by hydrophobic interactions, which becomes cooperative when the presence of surfactant is high enough. Finally, a plateau is observed, suggesting the saturation binding region.

**Determination of Aggregation Numbers.** With the aim of examining the effect of the protein on the micelle aggregation number of MEGA-10, we have used the well-established fluorescence static quenching method.<sup>19</sup> Vasilescu et al.<sup>20</sup> have applied both static and time-resolved methods for the determination of aggregation numbers of micellar aggregates formed in several protein–surfactant systems. The aforementioned authors have widely discussed the applicability of both methods to these systems. The main problem resides in the possibility that molecules of probe, quencher, and surfactant adsorb on the protein before the cooperative, aggregative adsorption. In addition, it is furthermore probable that molecules adsorbed in specific sites on the protein are transferred into the micelle-like aggregates. Because it was not possible to differentiate both situations, they calculated the aggregation numbers as if all surfactant, probe, and quencher were micellized. Under this assumption, they obtained comparable results by the application of both static and dynamic methods.<sup>20</sup> In our experiments of fluorescence static quenching, we used pyrene as a probe and CPyC as a quencher, as this pair ensures the fulfillment of the appropriate requirements for the application of this method.<sup>33</sup> The results of the quenching experiments were analyzed by using the following equation:

$$\ln \frac{I_0}{I} = \frac{N_{\text{agg}}}{[S] - \text{CMC}} [Q] \quad (7)$$

where  $I_0$  and  $I$  are the fluorescence intensities in the absence and presence of quencher, respectively,  $N_{\text{agg}}$  is the mean aggregation number,  $[S]$  is the total surfactant concentration, and  $[Q]$  is the quencher concentration. The fluorescence intensities at 383 nm were plotted according to eq 7 (plots not shown), and an acceptable linear relationship ( $r > 0.99$ ) was observed in all the cases. From these plots, and by using the CMC values previously determined, we have obtained the  $N_{\text{agg}}$  values in aqueous medium and in the presence of 1% BSA. It is to be noted that the  $N_{\text{agg}}$  value that we have obtained in aqueous medium ( $74 \pm 1$ ) agrees well with the literature values.<sup>34,35</sup> In addition, we have found that the  $N_{\text{agg}}$  value in the presence of 1% BSA is considerably reduced ( $46 \pm 1$ ). Similar results were obtained by Vasilescu et al. in several protein–surfactant systems, including those constituted by the nonionic surfactant C<sub>12</sub>E<sub>8</sub> and the proteins BSA and lysozyme.<sup>20</sup> In studies dealing with polymer–surfactant systems, a decrease in the aggregation number as compared to the value of the surfactant water system is generally reported, this change being considered as a strong indication of a polymer–surfactant interaction.<sup>36</sup> In our case, it seems clear that the  $N_{\text{agg}}$  value that we have obtained in the presence of protein represents an average value of two types of aggregates: the free micelles and the micelle-like aggregates adsorbed, by hydrophobic interactions, onto the surface protein. According to this picture, we can assume a necklace structure for the protein–surfactant complex,<sup>10</sup> where the micellar clusters, smaller than the free micelles, are adsorbed on the surface of the protein polypeptidic. This binding mechanism is probably accompanied by some conformational change in the protein structure as a result of hydrophobic interactions.<sup>20</sup>

**Resonance Energy Transfer from Trp to ANS.** Resonance energy transfer (RET) can provide important structural and dynamic information on macromolecular assemblies.<sup>37</sup> In fact, RET studies have been used to characterize several aspects in macromolecule–ligand complexes, including polymer–surfactant<sup>38</sup> and protein–surfactant systems.<sup>28,37</sup>

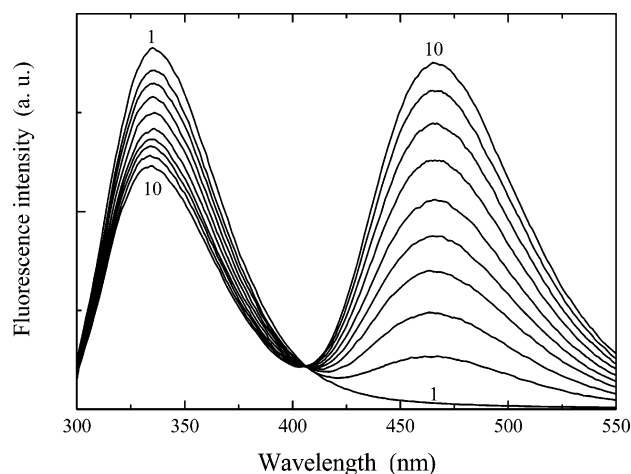


**Figure 5.** Fluorescence spectra of BSA solutions (30  $\mu\text{M}$ ) in 20 mM MEGA-10 and varying concentrations of ANS: 1  $\rightarrow$  0 mM and 10  $\rightarrow$  0.15 mM ( $\lambda_{\text{exc}}$  = 295 nm).

The RET process occurring by dipolar interactions is described by the Förster theory.<sup>39</sup> According to Förster's approach, the rate constant for RET,  $k_{\text{ET}}$ , due to a dipole–dipole interaction mechanism, is dependent upon the donor–acceptor distance,  $R$ , by the equation

$$k_{\text{ET}} = \frac{8.8 \times 10^{-25} K^2 \Phi_D}{n^4 \tau_D R^6} J \quad (8)$$

where  $K^2$  is a factor describing the relative orientation in space of the transition dipoles of donor and acceptor,  $n$  is the refractive index of the medium,  $\tau_D$  and  $\Phi_D$  are the lifetime and quantum yield for the donor in the absence of the acceptor, and  $J$  is the spectral overlap integral between donor emission and acceptor absorption. From eq 8, it is evident that there is a strong dependence of the RET process on the distance  $R$ ; hence, RET studies are especially useful to estimate changes in the separation distance between donor and acceptor. On the other hand, it is also observed from eq 8 that  $k_{\text{ET}}$  depends directly on the spectral overlap integral. Therefore, the RET process requires a significant overlap between donor emission and acceptor absorption spectra. Since the emission spectra of Trp shows a good overlap with the absorption spectra of ANS, the RET between them is possible. In fact, this donor–acceptor pair recently has been used to examine several protein–surfactant systems.<sup>28</sup>

We have also studied the effect of the surfactant addition on the RET from Trp to ANS in the BSA/MEGA-10 system. Figure 5 shows the combined spectra of the Trp–ANS pair in a system with a fixed protein concentration (30  $\mu\text{M}$ ) and increasing ANS concentrations and in the presence of 20 mM MEGA-10. From these spectra, it can be seen that as the ANS concentration increases, the quenching of Trp occurs accompanied by successive enhancement in ANS fluorescence. Figure 6 shows the effect of the surfactant concentration on the efficiency in the RET process between Trp and ANS as followed by the acceptor fluorescence enhancement. From this figure, it is observed that at a low surfactant concentration (2 mM), the RET process is unaffected, indicating that the distance between donor and acceptor remains invariable, and what can be interpreted is that at this surfactant concentration, which is below the CMC, the binding of surfactant to protein occurs without alterations in the protein structure. However, when the surfactant concentration rises above the CMC (20 mM), a significant reduction in the efficiency of the RET process it is observed, indicating a

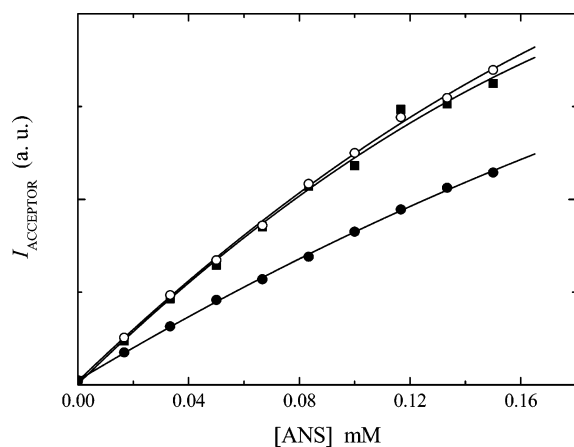


**Figure 6.** Enhancement of ANS emission as a function of its concentration at different surfactant concentrations: (■) 0 mM, (○) 2 mM, and (●) 20 mM.

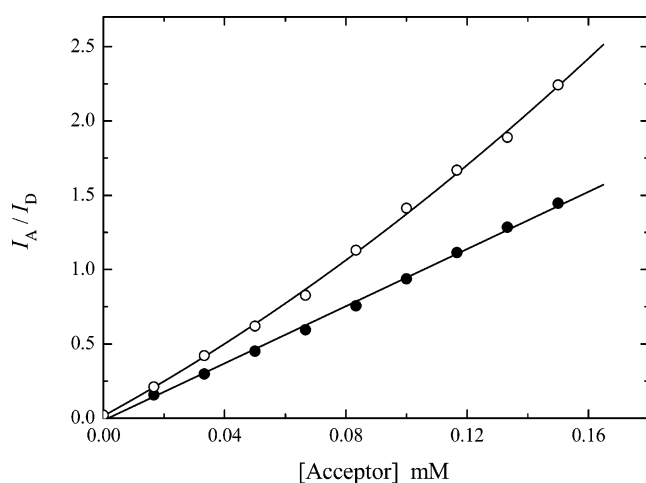


**Figure 7.** Intensity ratio of ANS emission to Trp emission as a function of ANS (acceptor) concentration at different surfactant concentrations: (○) 2 mM and (●) 20 mM.

greater separation between donor and acceptor. This fact can be related to some change in the protein structure, leading to a slight increase in the initial size.

On the other hand, it has been established that if the distribution of donor and acceptor follows a Poisson distribution among surfactant clusters on the polymer, the treatment proposed by Atik et al.<sup>40</sup> applies, and the following equation can be deduced:<sup>38</sup>

$$\frac{I_A}{I_D} = \frac{\Phi_A}{\Phi_D} \frac{[A]}{[\text{cluster}]} \quad (9)$$

where  $I_A$  and  $I_D$  are the fluorescence intensities of acceptor and donor, respectively,  $\Phi_A$  and  $\Phi_D$  are the corresponding fluorescence quantum yields,  $[A]$  is the acceptor concentration, and  $[\text{cluster}]$  stands for the concentration of surfactant clusters. Therefore, from the slope of a plot of  $I_A/I_D$  against the acceptor concentration, the cluster concentration,  $[\text{cluster}]$ , can be obtained. To check the validity of eq 9 for the BSA/MEGA-10 system, the corresponding RET data have been plotted in Figure 7. From this figure, it is observed that at a low surfactant concentration (2 mM), the experimental data are better fitted to a second-order polynomial, whereas at a high surfactant concentration, an excellent linear fit ( $r = 0.999$ ) is found. From this result, it could be concluded that the formation of surfactant clusters only occurs at a high surfactant concentration, where

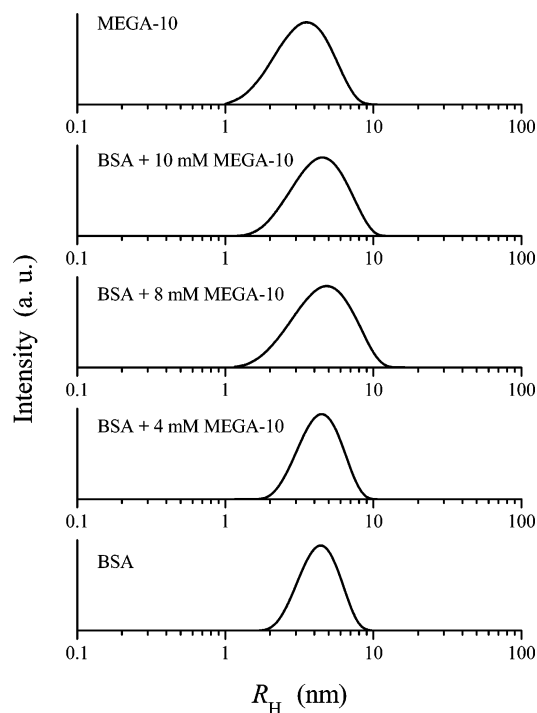


**Figure 8.** Hydrodynamic radii distribution from dynamic light scattering measurements carried out with solutions of constant protein concentration, 30  $\mu\text{M}$ , and increasing surfactant concentrations for the BSA/MEGA-10 system.

the model represented by eq 9 describes the experimental results well. From the slope of the linear plot in Figure 7, and by using the literature values for  $\Phi_A$  and  $\Phi_D$  ( $\Phi_A = 0.7$  and  $\Phi_D = 0.044$ ),<sup>28</sup> we have obtained a value of 1.7 mM for  $[\text{cluster}]$ . Nevertheless, taking into account the surfactant concentration used (20 mM), this surfactant cluster concentration implies less than 10 surfactants per cluster. Since the protein concentration used in these experiments was 30  $\mu\text{M}$ , there should be above 500 clusters per BSA. Obviously, the application of eq 9 to the present case provides nonrealistic estimates of aggregation numbers of surfactant clusters. We think that this fact may be due to the occurrence of energy transfer between a donor (Trp), which is built in the protein, and different acceptors (ANS), solubilized in adjacent clusters bound to the protein. From a qualitative point of view, one can assume, however, that the observed effective energy transfer is indicative of highly cooperative binding systems inducing large surfactant aggregates. According to this view, our RET data are consistent with the binding model proposed previously. That is, at a low surfactant concentration, a non-cooperative binding, controlled by hydrophobic interactions, takes place. In this stage, the protein structure does not undergo significant structural changes. Next, as the surfactant is added, the surfactant–protein binding is characterized by a process cooperative in nature, where some surfactant clusters should be adsorbed on the protein surface, leading to the formation of “pearl necklace” complexes coexisting with the free micelles of the surfactant.

**Dynamic Light Scattering Studies.** To obtain additional information on the protein–surfactant binding process, we have carried out dynamic light scattering measurements on mixed solutions of BSA and MEGA-10, keeping the concentration of protein constant (30  $\mu\text{M}$ ) and adding increasing amounts of surfactant. Figure 8 shows the distribution of intensities as a function of the apparent hydrodynamic radius of BSA alone and in the presence of increasing concentrations of MEGA-10. For comparison, we have also included in Figure 8 the



corresponding plot for the surfactant alone. First of all, it is to be noted from Figure 8 that BSA and MEGA-10 micelles have similar sizes (4.3 nm for BSA and 3.9 nm for MEGA-10). The analysis of the mixed systems reveals a unimodal distribution of aggregates, which increase slightly in size when the surfactant concentration rises above the CMC. However, the fact that the distribution patterns of the protein alone and with 4 mM MEGA-10 (below the CMC) are rather identical is remarkable. Note that this result suggests that the protein structure is unaffected by the surfactant binding, in good agreement with our results from RET studies. On the other hand, the unimodal distribution observed when the surfactant concentration is above the CMC (8 and 10 mM MEGA-10) is wider than that of BSA alone, and its size is slightly bigger than that of both the pure protein and the free MEGA-10 micelles. This fact could be explained by assuming that at surfactant concentrations above the CMC, the system is constituted of two species: (i) the protein-surfactant complexes, with a size slightly greater than that of BSA, due to the conformational changes induced by the adsorption of the surfactant<sup>20</sup> and (ii) the free micelles of the surfactant, which should be formed once the saturation condition in the binding process of the surfactant to the protein is raised.

### Conclusion

Through the present study of mixed systems constituted by the protein BSA and the nonionic surfactant MEGA-10, by using surface tension, fluorescence spectroscopy, and dynamic light scattering measurements, we have obtained strong indications of the binding between them. The binding studies that we have performed by two different methods suggest a cooperative binding controlled by interactions of a hydrophobic character. The results that we have obtained on the effect of protein on the aggregation numbers indicate the formation of micelle-like aggregates, smaller than the free micelles, adsorbed on the protein surface. We have demonstrated that the efficiency of the RET process between Trp residues and ANS is reduced in the presence of a high surfactant concentration, which has been interpreted in the sense that the binding of the surfactant on the protein produces some conformational alteration in its structure. From these results, a conceptual scheme based on the so-called "necklace and bead" model has been proposed. Although our dynamic light scattering studies are not conclusive, because we could not discriminate between free micelles and protein-surfactant complexes, the results that we have obtained can be explained in light of the previous model.

**Acknowledgment.** This work was financially supported by the Spanish Science and Technology Ministry (Project CTQ2005-04513).

### References and Notes

- (1) Dalgleish, D. G. In *Emulsions and Emulsion Stability*; Sjöblom, J., Ed.; Marcel Dekker: New York, 1996; Ch. 5.
- (2) Peters, T., Jr. *All About Albumin Biochemistry, Genetics, and Medical Applications*. Academic Press: San Diego, CA, 1996.
- (3) Sjögren, H.; Ericsson, C. A.; Evenäs, J.; Ulvenlund, S. *Biophys. J.* **2005**, *89*, 4219.
- (4) Ananthapadmanabhan, K. P. In *Interactions of Surfactants with Polymers and Proteins*; Goddard, E. D., Ananthapadmanabhan, K. P., Eds.; CRC Press Inc.: Boca Raton, FL, 1993; Ch. 8.
- (5) Rodenhiser, A. P.; Kwak, J. C. T. In *Polymer-Surfactant Systems, Surfactant Science Series*, Vol. 77; Kwak, J. C. T., Ed.; Marcel Dekker: New York, 1998; Ch. 1.
- (6) Garavito, R. M.; Ferguson-Miller, S. *J. Biol. Chem.* **2001**, *276*, 32043.
- (7) Turro, N. J.; Lei, X.-G.; Ananthapadmanabhan, K. P.; Aronson, M. *Langmuir* **1995**, *11*, 2525.
- (8) Ghosh, S.; Banerjee, A. *Biomacromolecules* **2002**, *3*, 9.
- (9) Das, R.; Guha, D.; Mitra, S.; Kar, S.; Lahiri, S.; Mukherjee, S. *J. Phys. Chem. A* **1997**, *101*, 4042.
- (10) Guo, X.-H.; Chen, S.-H. *Chem. Phys.* **1990**, *149*, 129.
- (11) Valstar, A.; Vasilescu, M.; Vigouroux, C.; Stilbs, P.; Almgren, M. *Langmuir* **2001**, *17*, 3208.
- (12) Stenstam, A.; Khan, A.; Wennerström, H. *Langmuir* **2001**, *17*, 7513.
- (13) Deo, N.; Jockusch, S.; Turro, N. J.; Somasundaram, P. *Langmuir* **2003**, *19*, 5083.
- (14) Sabín, J.; Prieto, G.; González-Pérez, A.; Ruso, J. M.; Sarmiento, F. *Biomacromolecules* **2006**, *7*, 176.
- (15) Cserháti, T. *Environ. Health Perspect.* **1995**, *103*, 358.
- (16) Hill, K.; Rhode, O. *Fett/Lipid* **1999**, *101*, 23.
- (17) Hildreth, J. E. K. *Biochem. J.* **1982**, *207*, 363.
- (18) Kalyanasundaram, K.; Thomas, J. K. *J. Am. Chem. Soc.* **1977**, *99*, 2039.
- (19) Turro, N. J.; Yekta, A. *J. Am. Chem. Soc.* **1978**, *100*, 5951.
- (20) Vasilescu, M.; Angelescu, D.; Almgren, M.; Valstar, A. *Langmuir* **1999**, *15*, 2635.
- (21) Aguiar, J.; Carpena, P.; Molina-Bolívar, J. A.; Carnero Ruiz, C. *J. Colloid Interface Sci.* **2003**, *258*, 116.
- (22) Nishikido, N.; Takahara, T.; Kobayashi, H.; Tanaka, M. *Bull. Chem. Soc. Jpn.* **1982**, *55*, 3085.
- (23) Tribout, M.; Paredes, S.; Gonzáles-Mañas, J. M.; Goñi, F. M. *J. Biochem. Biophys. Methods* **1991**, *22*, 129.
- (24) Nishiyama, H.; Maeda, H. *Biophys. Chem.* **1992**, *44*, 199.
- (25) Zadyanova, N. M.; Yampolckaya, G. P.; Filatova, L. Y. *Colloid J.* **2006**, *68*, 162.
- (26) Rosen, M. J. *Surfactants and Interfacial Phenomena*, 2nd ed.; Wiley: New York, 1989.
- (27) Andreu, J. M.; Muñoz, J. A. *Biochemistry* **1986**, *25*, 5220.
- (28) De, S.; Girigoswami, A.; Das, S. *J. Colloid Interface Sci.* **2005**, *285*, 562.
- (29) De, S.; Das, S.; Girigoswami, A. *Colloids Surf., B* **2007**, *54*, 74.
- (30) Pi, Y.; Shang, Y.; Peng, C.; Liu, H.; Hu, Y.; Jiang, J. *Biopolymers* **2006**, *83*, 243.
- (31) Lakowicz, J. R. *Principles of Fluorescence Spectroscopy*, 2nd ed.; Plenum: New York, 1999.
- (32) Jones, M. N. *Biochem. J.* **1975**, *151*, 109.
- (33) Kalyanasundaram, K. *Photochemistry in Microheterogeneous Systems*; Academic Press: New York, 1987.
- (34) Okawauchi, M.; Hagio, M.; Ikawa, Y.; Sugihara, G.; Murata, Y.; Tanaka, M. *Bull. Chem. Soc. Jpn.* **1987**, *60*, 2718.
- (35) Hierrezuelo, J. M.; Aguiar, J.; Carnero Ruiz, C. *Langmuir* **2004**, *20*, 10419.
- (36) Lindman, B.; Thalberg, K. In *Interactions of Surfactants with Polymers and Proteins*; Goddard, E. D., Ananthapadmanabhan, K. P., Eds.; CRC Press: Boca Raton, FL, 1993; Ch. 5.
- (37) Wu, P.; Brand, L. *Anal. Biochem.* **1994**, *218*, 1.
- (38) Hayakawa, K.; Nakano, T.; Satake, I.; Kwak, J. C. T. *Langmuir* **1996**, *12*, 269.
- (39) Förster, T. *Z. Naturforsch., A: Phys. Sci.* **1949**, *4*, 321.
- (40) Atik, S. S.; Nam, M.; Singer, L. A. *Chem. Phys. Lett.* **1979**, *67*, 75.

BM0704121